IJMOT

INTERNATIONAL JOURNAL OF MICROWAVE AND OPTICAL TECHNOLOGY

VOL. 1, NO. 1, JUNE 2006

Millimeter-Wave Photonic Techniques: Part III- Modulation and Demodulation Schemes and System Integration Based on Substrate Integrated Circuits

Xiupu Zhang[1], Ke Wu[2], Jianping Yao[3], and Raman Kashyap[2, 4]

[1] Department of Electrical and Computer Engineering
Concordia University, Montreal, Canada

[2] Poly-Grames Research Center, Department of Electrical Engineering
Ecole Polytechnique de Montreal, Montreal, Canada

[3] Microwave Photonics Research Laboratory
School of Information Technology and Engineering
University of Ottawa, Ottawa, Canada

[4] Department of Engineering Physics
Ecole Polytechnique de Montreal, Montreal, Canada

***Abstract*-The techniques to implement radio over fiber (RoF) systems using optical subcarrier modulation (SCM) and dense wavelength division multiplexing (DWDM) are reviewed, which include the techniques of SCM, millimeter-wave (mm-wave) generation and reception at base stations, and optical multiplexing/demultiplexing. The impact of system nonlinear distortions and their suppression are also reviewed. In addition, the integration of the future mm-wave photonic systems based on substrate integrated circuits (SICs) is discussed. Some examples of system on substrate or on chip are provided.**

***Index Terms*- radio over fiber, millimeter-wave, dense wavelength division multiplexing, subcarrier modulation broadband wireless access, substrate integrated circuits**

I. INTRODUCTION

In a radio over fiber (RoF) system, optical subcarrier modulation (SCM) is usually used to multiplex multiple channels of millimeter-wave (mm-wave) signals on an optical carrier for broadband wireless access. In addition, the use of SCM scheme will also facilitate the generation of mm-wave signals at base stations (BSs). To increase the area of coverage and the communication capacity, dense wavelength division multiplexing (DWDM) technique should be employed in an mm-wave RoF system. The RoF systems can be implemented using commercially-available discrete devices. The key challenges in applying the mm-wave photonic techniques for practical applications are the large system footprint and high system cost. A solution to the problems is to use the innovative substrate integrated circuits (SICs). It is expected that a complete mm-wave photonic system can be integrated on the same substrate to realize the subsystem-on-substrate or system-on-substrate for mm-wave photonic applications. In this paper, we will first review some new techniques developed recently about optical SCM, optical multiplexing/demultiplexing of mm-wave band subcarrier modulated optical carriers, mm-wave generation and reception of mm-wave signals at BSs, and the impact of nonlinear distortions and the techniques for nonlinearity suppression. Then, the design challenges of future mm-wave photonic systems using the state-of-the-art SIC techniques are discussed. Some design examples of system-on-substrate or -chip are provided.

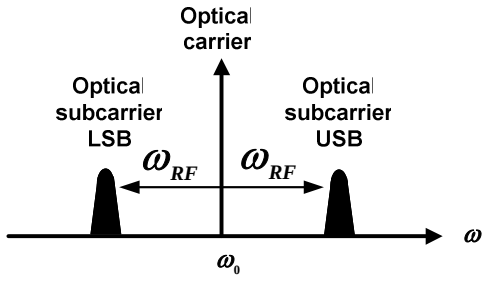

Fig. 1. Spectrum for an optical light with SCM by direct modulation of a laser or external modulation with RF of ω_{RF}. ω_0 is the central frequency of the optical light.

II. MODULATION AND DEMODULATION SCHEMES BASED ON DWDM TECHNIQUE

A. Optical Subcarrier Modulation

An optical carrier can carry a sinusoidal RF tone and the RF sinusoidal tone can be modulated by a digital electrical signal. Thus there are two carriers, and one is the optical carrier and the other is the RF carrier which is referred to as the subcarrier in the optical domain. Transmission of an optical carrier with its subcarrier over fiber is referred to as RoF, or optical analog transmission. Practically, it is straightforward to obtain optical SCM that a RF signal directly drives the current of a laser diode or modulation voltage of an external modulator, where the modulation response of the laser diode or the external modulator must be broader than the RF carrier frequency. The optical spectrum of a laser diode or an external modulator with SCM is shown in Fig. 1. It is seen that there are two optical subcarriers, separated by ω_{RF} in frequency from the optical carrier, where ω_{RF} is the frequency of the RF carrier. Because of two subcarriers, it is referred to as double sideband (DSB) SCM, with a upper sideband (USB) and a lower sideband (LSB). When ω_{RF} is in mm-wave band, for example, from 30 to 60 GHz, the modulation response of the laser diode or the external modulator must have a 3-dB bandwidth of at least ω_{RF}. Laser diodes and optical modulators with 3-dB bandwidth of the range of mm-wave band are very expensive presently, particularly for the laser diodes. For external modulation, two types of modulators are commonly used: optical Mach-Zehnder modulators (MZMs) and electro-absorption modulators (EAMs).

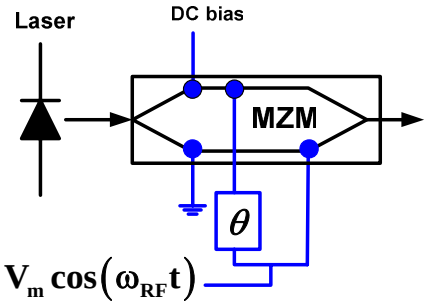

Fig. 2. Schematic of using an MZM for an optical carrier carrying a RF signal with SSB SCM.

As shown in Fig.1, two subcarriers may carry the same RF signal. Thus fiber chromatic dispersion induced power penalty is introduced since the two subcarriers, separated by tens of GHz, have a large walk-off after fiber transmission. When the phase difference of the two subcarriers after fiber transmission is π, direct photodetection of the two subcarriers with the optical carrier will completely cancel out the RF signal. To reduce fiber chromatic dispersion, a straightforward way is to use a single sideband (SSB) SCM. Thus the chromatic dispersion introduced walk-off between the two subcarriers is avoided. A simple technique to obtain SSB SCM is to use an optical notch filter to remove one of the two subcarriers after optical SCM. The other technique of SSB SCM generation is to use external modulation with a dual-port MZM [1] as shown in Fig. 2, where $\theta = \pm\pi/2$. When $\theta = +\pi/2$ $(-\pi/2)$ is used, the LSB (USB) subcarrier will be shown up only in Fig. 1. To improve the optical spectral efficiency, one optical carrier should carry multiple optical subcarriers and each subcarrier conveys its own RF signal. As an example, we consider an optical carrier of transporting two subcarriers. When SSB SCM is used two RF signals at Ω_1 and Ω_2 drive the two arms of the MZM, and one branch has a phase shift of $\theta = \pm\pi/2$, as shown in Fig. 2. The electric field after SCM is given by

$$E(t)=\frac{A}{\sqrt{2}}\begin{Bmatrix}\sqrt{2}J_0^{\,2}(\xi\pi)\cos\left(\omega_0 t+\frac{\pi}{4}\right)\\ -2J_0(\xi\pi)J_1(\xi\pi)\cos(\omega_0 t\mp\Omega_1 t)\\ -2J_0(\xi\pi)J_1(\xi\pi)\cos(\omega_0 t\mp\Omega_2 t)+\cdots\end{Bmatrix} \quad (1)$$

where the sign of $\mp$ corresponds to $\theta=\pm\pi/2$. It is seen that the two subcarriers are located either in LSB or in LSB. In (1), $J_n(\ )$, n = 0, and 1, is the Bessel function of the first kind, and $\xi=V_m/V_\pi$ is optical modulation index (OMI), where V_m and V_π are the modulation and π voltages of the MZM.

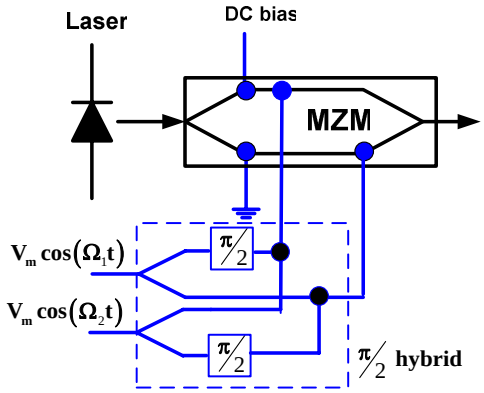

Fig. 3. Schematic of using an MZM for an optical carrier carrying two RF signals with TSSB SCM [2].

Alternatively, the two subcarriers can be located in tandem of the optical carrier, i.e. tandem SSB (TSSB) SCM. To obtain TSSB SCM, two RF signals, at Ω_1 and Ω_2, drive a four port 90^0 hybrid. The two hybrid outputs drive a dual-port MZM, biased at the quadrature [2], as shown in Fig. 3. The electric field after optical modulation

$$E(t)=\frac{A}{\sqrt{2}}\begin{Bmatrix}\sqrt{2}J_0^{\,2}(\xi\pi)\cos\left(\omega_0 t+\frac{\pi}{4}\right)\\ -2J_0(\xi\pi)J_1(\xi\pi)\cos(\omega_0 t+\Omega_1 t)\\ -2J_0(\xi\pi)J_1(\xi\pi)\sin(\omega_0 t-\Omega_2 t)\\ +\cdots\end{Bmatrix} \quad (2)$$

It is seen that the subcarriers at Ω_1 and Ω_2 are located in the USB and LSB, respectively.

One important parameter in SCM generation is OMI $\xi=V_m/V_\pi$, which determines the magnitude of the subcarriers with respect to the optical carrier. A larger OMI will induce a larger magnitude of the subcarriers. A larger subcarrier will relatively reduce the impact of laser's relative intensity noise and receiver's thermal noise when the subcarrier and its optical carrier are photodetected. Intuitively, a larger OMI is preferable. However, a larger OMI would introduce nonlinear distortion due to nonlinear response of the modulator. The nonlinear distortion will induce crosstalk and degrade the signal to noise ratio (SNR). The nonlinear distortion can be resulted from the nonlinear modulation response of laser diodes, optical modulators, optical receivers and other optical components in a RoF system, particularly nonlinear modulation response. Consequently, a small OMI is usually used to avoid serious nonlinear distortions.

B. Optical Multiplexing and Demultiplexing

When mm-wave RoF systems are incorporated with DWDM technique, how to optically multiplex and demultiplex multiple optical wavelengths becomes a technical issue when the mm-wave subcarrier frequency is beyond the conventional DWDM channel spacing. In other words, when the channel spacing is 100 GHz or beyond, the optical carrier and its subcarriers can be within the passband of the conventional optical multiplexers and demultiplexers. Thus commercially-available multiplexers and demultiplexers, which are widely used for current DWDM optical communications systems, can be applied to mm-wave RoF systems. However, when the channel spacing is 50 GHz or smaller, the commercially-available multiplexers and demultiplexers may not be applied directly to mm-wave RoF systems, because the frequency interval between the optical carrier and its subcarriers is beyond the channel spacing, and thus the bandwidth of the optical filters of the optical multiplexers and demultiplexers.

A straightforward method to overcome the problem is to modify the optical multiplexers and

demultiplexers [3], as shown in Fig. 4. Optical interleaved optical carriers and their subcarriers arrive at an optical circulator, one arm of which is connected to a high-finesse Fabry Perot (FP) etalon. All optical carriers pass through the FP etalon and all subcarriers are reflected to the optical circulator. Finally the each optical carrier and its subcarrier are recombined and sent out to the port of the demultiplexer. Similarly, optical multiplexing implementation is just reversed process to Fig. 4. Polarization maintaining of multiplexing and demultiplexing must be used.

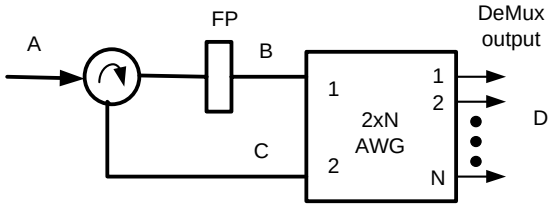

Fig. 4. A demultiplexer of DWDM mm-wave RoF systems [3].

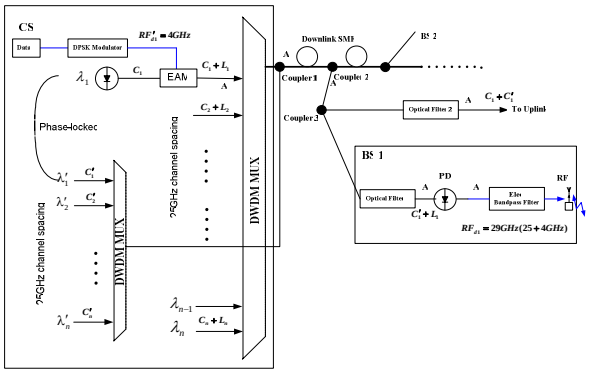

Fig. 5. DWDM mm-wave RoF downlink system with a channel spacing of 25 GHz and a RF of 29 GHz [4].

Recently, we proposed a novel technique without using optical interleaving, but conventional DWDM multiplexers and demultiplexers are used [4]. For illustrations we consider a DWDM RoF system with a channel spacing of 25 GHz and a RF carrier downlink/uplink frequency of 29/27 GHz with bus topology. Fig. 5 shows the schematic of the downlink system. There are a total of n optical channels or carriers, i.e. $C_1, C_2, C_3, \cdots, C_n$, or in terms of wavelengths $\lambda_1, \lambda_2, \lambda_3, \cdots, \lambda_n$. In this illustration we only consider each optical carrier transporting one subcarrier, located at the LSB of the optical carrier. The LSB subcarrier can be obtained by using an EAM driven by a RF signal with a low RF, RF'_{d1}, as shown in Fig. 1. For example, consider RF'_{d1} = 4 GHz, thus the total occupied bandwidth including the optical carrier and subcarrier is ~4 GHz for each channel, far below the channel spacing of 25 GHz. Therefore, conventional optical multiplexers can be used for this downlink system. Moreover, an EAM with 3-dB bandwidth of around 4 GHz can be used, rather than an EAM with mm-wave bandwidth. There is the other set of optical carriers, i.e. $C'_1, C'_2, C'_3, \cdots, C'_n$ or in terms of wavelengths $\lambda'_1, \lambda'_2, \lambda'_3, \cdots, \lambda'_n$, which are CW and 25-GHz shorter in wavelength (or higher in frequency). They are optically multiplexed and coupled together with the first set of optical channels as shown in Fig. 5. Suppose that the optical carriers λ_1 and λ'_1, λ_2 and λ'_2, and so on, are phase-locked, respectively; and the two optical carriers (i.e. λ_1 and λ'_1, λ_2 and λ'_2, and so on) are polarization-aligned respectively until they are combined together. The two groups of optical sources can be implemented by a supercontinuum light source [5], in which all wavelength modes are phase-locked, or carrier suppression modulation generated two lights. After optical multiplexing and combiner 1, the optical spectrum is shown in Fig. 6. The polarization alignment is shown in the same color in Fig. 6. It is observed that no optical interleaving occurs. After fiber transmission, optical filter 1 is used to extract the optical carrier C'_1 and the subcarrier L_1, resulting in the optical spectrum shown in Fig. 6 (within dashed lines) and photodetection for generating a 29-GHz RF signal. Accordingly, all other BS's have the similar configuration as in BS 1. Another optical filter (i.e. optical filter 2) is utilized to extract the optical carriers C_1 and C'_1, used for the uplink system. As a result, the ~4-GHz RF carrier at the central station (CS) is up-shifted to a ~29-GHz RF signal at each BS. Compared to the conventional coherent heterodyne detection, the optical carrier C'_1 acts

as the local optical oscillator for the subcarrier L_1. Moreover, because the optical carriers C_1', and C_1 are phase-locked, the downlink system is immune to the laser phase noise.

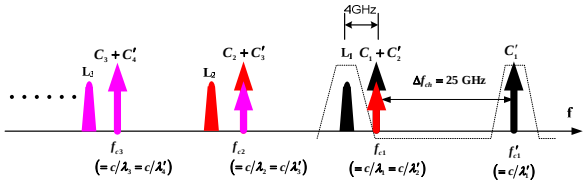

Fig. 6. Optical spectrum after optical combiner 1, i.e. at point A2 in Fig. 5. The dashed line indicates optical filter 1 in Fig. 5.

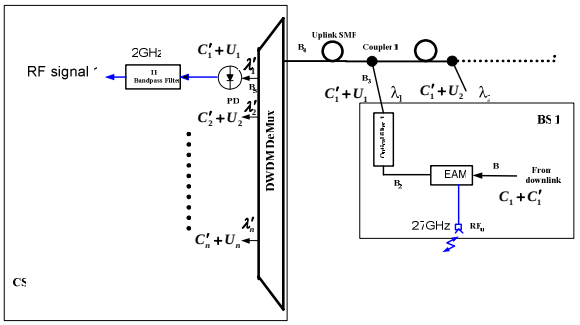

Fig. 7. Schematic showing the uplink of the proposed mm-wave RoF system [4].

The uplink of the proposed system is illustrated in Fig. 7. To simplify the BSs and reduce maintenance of the BSs, the technique of remote local optical oscillators is used. In other words, the optical carriers with the optical wavelengths λ_1 and λ_1' are used for both downlink and uplink for the connection between the CS and BS 1. The ~27-GHz RF signal, which is received from an antenna, is imposed onto the two optical carriers C_1 and C_1' simultaneously by using a polarization-insensitive EAM as shown in Fig. 7 at BS 1. Thus, each of optical carriers C_1 and C_1' has two optical subcarriers; and an optical filter (i.e. optical filter 1 in Fig. 7) simply filters out the optical carrier C_1' and the subcarrier U_1, which is a subcarrier of the optical carrier C_1; therefore the optical carrier C_1' becomes the new optical carrier for the subcarrier U_1. Then, the optical carrier C_1' and the subcarrier U_1 are coupled into the uplink transmission fiber. Optical filtering also reduces non-adjacent channel crosstalk. Because the frequency difference between the optical carrier C_1' and the subcarrier U_1 is ~2 GHz, the conventional DWDM demultiplexer can be directly applied to extract each optical carrier together with its subcarrier. Moreover, frequency interleaving is not used, and thus OSNR penalty and OMI degradation due to the frequency interleaving are not introduced. The optical spectrum at the input of the DWDM demultiplexer is shown in Fig. 8.

C. Millimeter-Wave Generation and Reception at Base Stations

We first consider mm-wave generation in downlink systems at BSs. In Figs. 5 and 6, we proposed a novel technique with remote local optical oscillators which are located in the CS for the generation of mm-wave RFs at BSs. At BSs the photodetection of the remote local optical oscillator and the subcarrier will directly generate a RF signal at mm-wave band. The magnitude of mm-wave RF can be tuned by changing the wavelength of the local optical oscillator and the RF of the subcarriers. When the channel spacing of 25 GHz is used, the direct generation of ~26-~60 GHz can be obtained. This technique was verified experimentally [5].

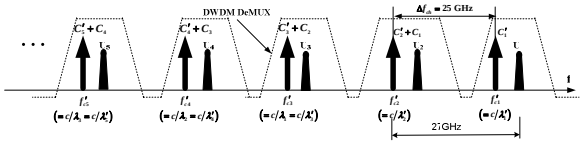

Fig. 8. Optical spectrum before the optical de-multiplexer, i.e. point B4 in Fig. 7.

An alternative technique for generating mm-wave in a downlink RoF system with a remote RF carrier was proposed [6]. For DWDM channel spacing of 25 GHz, each light carries four RF subcarriers at 7, 10, 13, 16 and a RF tone at 23 GHz. At each BS, the optical carrier and its all subcarriers are extracted by optical filtering. Then a second optical filter is used to separate the RF subcarriers from the RF tone, one half of the optical carrier with its four RF subcarriers and the other with the RF tone. After

photodetection, a local RF tone of 23 GHz is generated at BSs; and the four RF carriers are obtained by the other photodetection. With electrical mixing, the four RF carriers are up-converted into 30, 33, 36 and 39 GHz. If a further up-conversion is required an additional local electrical oscillator at RF of around several GHz is used.

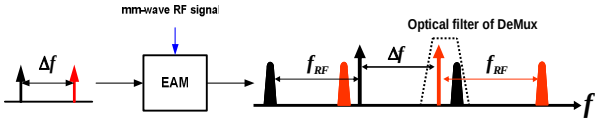

Fig. 9. Frequency down conversion with two optical carries into an EAM, driven by an mm-wave signal [4].

A third technique for generating mm-wave at BSs in the RoF downlink systems is based on a phase modulator [7] and direct photodetection. A light is modulated with a phase modulator at frequency of $f_{RF}/2$. Thus two optical subcarriers at $\pm f_{RF}/2$ are created. The optical carrier is removed by an optical notch filter and only the two subcarriers, separated by f_{RF} are left, which are used for two optical carriers. The two optical carriers are modulated by baseband signal. Thus, the same data is imposed onto the two optical carriers. By photodetection of the two optical carriers, a RF signal at f_{RF} is generated. For this technique DWDM channel spacing must be larger than f_{RF}. The phase modulator can be replaced by an MZM with carrier suppression modulation, but suffering from bias drifting.

Now we consider mm-wave reception at BSs. For the uplink systems, an antenna receives mm-wave signals which are sent to the CS. To use current DWDM multiplexers and demultiplexers, a simple technique was recently proposed [4], in which two lights, phase-locked and polarization-aligned, are input into an EAM, driven by a mm-wave RF signal at f_{RF}. Due to DSB SCM, each light has two subcarriers. One light (red) is only a few GHz away from the USB subcarrier of the other light (black). Thus, by optical filtering frequency down conversion is obtained as shown in Fig. 9.

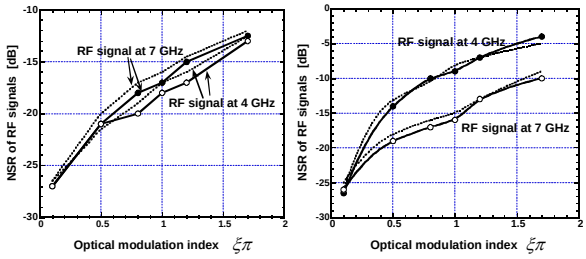

Fig. 10. NSR vs. OMI for RF signals at Ω_1 = 4 and Ω_2 = 7 GHz after fiber transmission of L = 50 km using (a) TSSB and (b) SSB SCM. Black (dotted) line indicates simulated (calculated) NSR [11].

A second technique of down conversion is based on the use of optical carrier suppression modulation [8]. Recently, this technique is simplified by using SCM proposed by us [9].

Another technique for an uplink mm-wave RoF system was recently proposed [10], where remote light located at the CS is sent to a BS and used for the uplink optical carrier, and the remote light carries an mm-wave RF tone with SCM. The detected mm-wave RF will be mixed with the uplink RF carrier to generate a radio signal with an IF.

C. Impact of Nonlinear Distortion and Suppression

As mentioned before, nonlinear modulation response will result in harmonic distortions (HDs) and intermodulation distortions (IMDs), due to SCM generation. As an example, we consider a case of a RoF system using TSSB SCM with an MZM. The two optical subcarriers carry two different RF signals, which are located at 4 and 7 GHz around the optical carrier. We use noise to signal (NSR) of after photodetection where nonlinear distortion within 12 GHz optical bandwidth and electrical 2-GHz bandwidth is included. Calculated and simulated NSR is shown in Fig. 10(a) for TSSB SCM [11]. Corresponding to Fig. 10(a), Fig. 10(b) shows NSR for a RoF system using SSB SCM with two subcarriers at 4 and 7 GHz. It can be seen that nonlinear distortion is increased with the increase of OMI. In other words, for a larger OMI nonlinear distortion will limit the performance of

a RoF system. Therefore, how to reduce the impact of nonlinear distortions in RoF systems is critical.

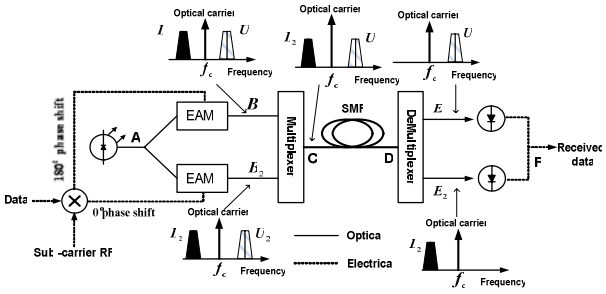

Fig. 11. Schematic of a balanced RoF system [12].

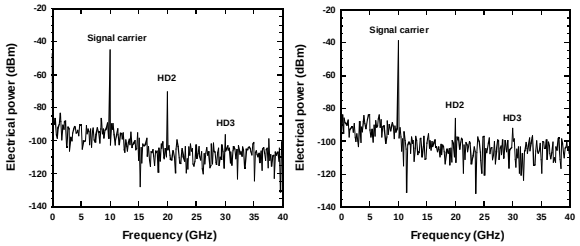

(a) (b)

Fig. 12. Electrical spectra obtained from (a) a non-balanced system and (b) balanced system. For the two systems, SCM at RF=10 GHz is considered [12].

Fig. 11 shows a balanced system which can suppress second-order HDs and IMDs [12]. Suppose that the two EAMs have the same modulation characteristics at a given wavelength. The two EAMs, biased at a voltage to reduce third-order HD, are driven by a RF signal with the lower branch having a 180^0 phase shift. By SCM, two optical subcarriers, i.e. LSB and USB are generated in each branch as shown in Fig. 11. After the multiplexer the optical carrier, LSB L_2 and USB U_1 are launched into transmission fiber. After fiber transmission an optical demultiplexer separates the USB U_1 and LSB L_2 along with half of the optical carrier. Each of USB and LSB with optical carrier is sent to one of balanced photodetectors to recover the electrical data. We consider a RF of 10 GHz. A single-mode fiber of 25 km was used with a chromatic dispersion of 16 $ps/(nm \cdot km)$. Fig. 12 shows simulated electrical spectra of RoF systems without balanced detection (Fig. 12(a)) and with balanced detection (Fig. 12(b)).

The other techniques to reduce modulation induced nonlinear distortion are to use either pre-distortion [13] or a linear modulator [14].

III. LOW-COST SUBSTRATE INTEGRATED CIRCUITS FOR MILLIMETER-WAVE RoF APPLICATIONS

One of the critical hurdles in the development of microwave and mm-wave photonic systems is related to the design and integration of electro-optical devices that should be broadband and fully compatible with other mm-wave front-end components. Generally, traveling-wave devices are used to provide a phase velocity matching condition between electrical and optical signals that is able to offer such broadband characteristics. They are designed in the form of microstrip and coplanar waveguide on the top of multilayered electro-optical substrates. In this case, the other basic requirements for the traveling-wave structures are to provide low-loss microwave transmission and also efficient overlapping of electrical and optical fields within the active region of the guided-wave region.

However, the conventional electro-optical traveling structures are difficult or very often impossible to provide simultaneously broadband and high-efficient electro-optical modulation or demodulation functionality (quantum efficiency). This is partly because the planar structures are usually quite lossy at mm-wave frequencies. In addition, it is difficult for the structure to achieve simultaneously two matching conditions in the truly optimum design of electro-optical devices, namely, impedance matching in connection with electro-optical field matching, thus electro-optical conversion or quantum efficiency, and phase velocity matching that is concerned with the bandwidth. On the other hand, the mm-wave front-end components are usually designed and integrated in the form of either microstrip or coplanar geometry, which is not necessarily

attractive at those frequencies because of loss thus low-Q. Therefore, low-loss mm-wave transmission structures that are compatible with well-established low-cost planar processing technique are highly desirable.

A. Substrate Integrated Circuits

We have proposed and developed the concept of SICs, which can be effectively used for both electrical and optical waveguide structures as shown in Fig. 13. The basic principle of the SICs is to design or synthesize the usually conventional non-planar structures in the form of "planar circuits" so that the planar and "non-planar" structures can be made onto single substrate at low cost with the existing processing or manufacturing techniques. Of course, low-cost mm-wave circuits and systems can also be made in multilayer platforms in which planar and "non-planar structures" are fully integrated in a three-dimensional manner. The "non-planar" and planar integrated structures can be regarded as "volume-field circuits" and "surface-field circuits", respectively.

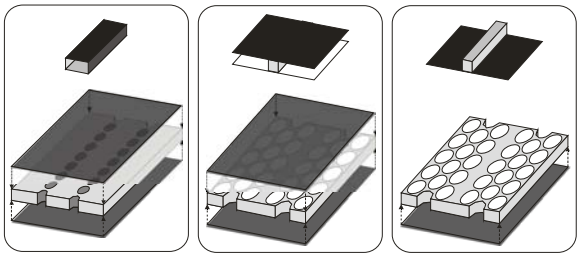

Fig. 13. General view of some SICs made on planar dielectric substrate (from left to right): SIW made of 2 rows of metallized holes, SINRD and SIIG, both made of air hole arrays.

Fig. 13 presents some typical SICs with the synthesized planar forms of metallic and dielectric waveguides that include substrate integrated waveguide (SIW), substrate integrated non-radiative dielectric (SINRD) guide, and substrate integrated image guide (SIIG) [15-19]. The techniques of synthesis make use of low-dielectric-filled holes that artificially create a dielectric guiding channel with the contrast of dielectric index, or a wave-confined guide with arrays of fence with metallized holes.

B. State-of-the-Art Development

A very large number of microwave and mm-wave SICs have been demonstrated with a series of low-cost fabrication techniques that include passive and active components as well as antennas. It has been found that the synthetic waveguides present modified properties due to the nature of periodic structures such as band-gap phenomena and existence of partial modes along the structures. Although simple design rules have been developed [15-24] and they are directly applicable in the construction of synthetic waveguides, some sophisticated simulation and analysis tools are always required. To design successful SICs, wideband and low-loss transitions between planar and non-planar structures are critical. Microstrip and coplanar waveguide (CPW) based high-quality transitions have been proposed. So far, the research results are still limited to some basic demonstrations of single passive/active SICs and integrated blocks such as filters, couplers, power dividers, diplexer-antenna units, mixers, oscillators, and others. Fig. 14 shows two SIW-based examples of realization.

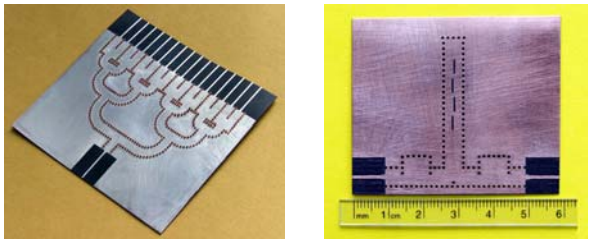

Fig. 14. Two realized SIW-microstrip examples (power divider and diplexer-antenna block).

In fact, main advantages of the SICs concept are still to be explored and demonstrated at the (sub) system level and a complete integration of front-end blocks should be done. Current results are essentially based on passive substrate techniques such as PCB and LTCC processes. No electro-optical devices have been studied and demonstrated yet so far on the basis of this perhaps revolutionary concept.

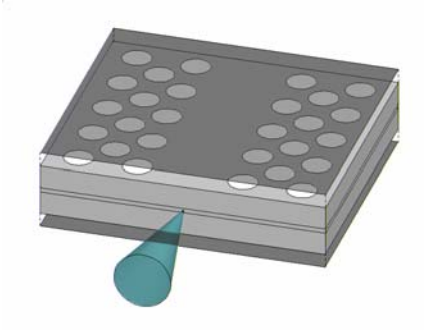

(a)

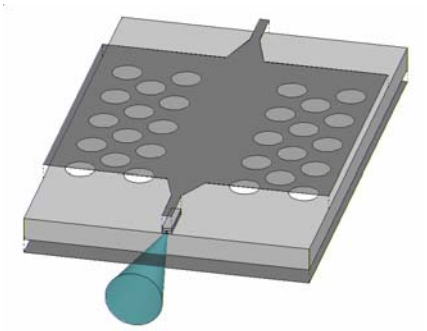

(b)

Fig. 15. Topologies of SINRD structures for electro-optical device applications: (a) PiN structure for detector or NiN structure for modulator, (b) Transition from waveguide photodiode to SINRD guide.

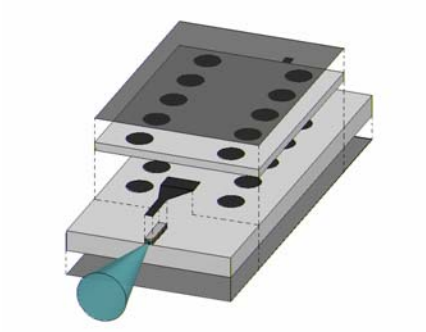

(a)

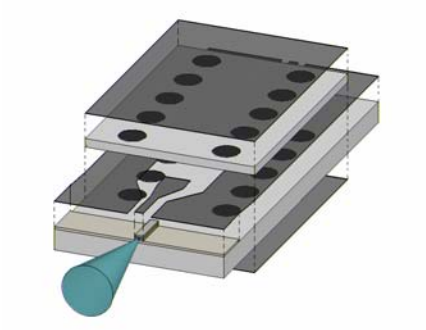

(b)

Fig. 16. Topologies of SIW structures for electro-optical device applications: (a) Transition from waveguide photodiode to SIW, (b) Transition from TWPD to SIW considering DC bias between dielectric layers.

It has been known that Si- and GaAs-based MMICs processing techniques are well developed for mm-wave applications. It is expected that the "non-planar" structures can also be synthesized into the semiconductor substrate, which become parts of the MMICs. Therefore, a series of high-quality passive and active circuits can be made onto single substrate including radiating elements (antennas) that are easily made with "non-planar" waveguides. As such, it is possible to develop a complete monolithic solution for designing mm-wave system front-ends as well as integrating them if necessary with the base-band signal processing unit if special platforms are used such as CMOS techniques. In addition, the synthetic semiconductor waveguides allow the development of innovative devices such as traveling-wave optoelectronic circuits. Low loss nano-structured techniques can also be used for a new class of ferrite components.

To illustrate the possibility of developing a system-on-substrate approach that allows the integration of complete mm-wave front-end blocks together with the traveling-wave electro-optical devices on the same multilayered electro-optical substrate, Figs. 15 and 16 show two proposed scenarios of fabricating traveling-wave electro-optical devices based on the SICs concept. It can be seen that the SICs concept can be used to synthesize basically all kinds of dielectric-based (or filled) waveguides by simply using air-holes (or other materials-filled holes in a general sense) and metallized holes. In our proposed electro-optical device integration with millimetre-wave front-ends, the SIC structures are effectively combined with the traveling-wave topologies with inherent electro-optical conversion or modulation/demodulation. In Fig. 15 (a), the multilayered semiconductor structure can be P-type, I-layer and N-type in order to

detect input light and convert it to electrical signal or can be N-, I and N+ layer to modulate input optical signal. Fig. 16 shows a possible integration scheme between photodetector and SIW structure. In Fig. 16(a), a waveguide photodetector is designed to absorb optical beam and multilayered SIW structure is then used to guide the converted millimetre-wave signal. In this structure, the top dielectric layer is deployed to separate DC bias and millimetre-wave signal in the device. In Fig. 16(b), traveling-wave photodetector (TWPD) design with broad bandwidth is considered instead of the conventional waveguide photodiode. In this scheme, the characteristic impedance of the TWPD is specified by CPW structure while the multilayered SIW excited by CPW is used as a low-loss transmission line.

With the SICs concept, there are countless possibilities in the design of electro-optical devices and millimetre-wave photonic circuits and systems. The ultimate goal is to design the complete system on the same substrate thus realizing the system-on-substrate or system-on-chip for mm-wave photonic applications.

IV. CONCLUSION

In this paper, we have reviewed the techniques of optical SCM, and mm-wave generation and reception at BSs based on DWDM in RoF networks. Optical multiplexing and de-multiplexing in RoF networks and the impact of nonlinear distortions and their suppression were also discussed. The potential of using SICs to implement system on substrate or -chip for future mm-wave RoF applications were also discussed.

ACKNOWLEDGMENT

The work is support by the Natural Sciences and Engineering Research Council of Canada, and the Canada Research Chairs Program (Wu and Kashyap).

The authors would like to acknowledge the contributions of Gang Zhou, Caiqin Wu, Baozhu Liu, and Biagio Masella of Concordia University, and Bouchaib Hraimel and Dominic Deslandes of Ecole Polytechnique de Montreal.

REFERENCES

[1] G. Smith, D. Novak, and Z. Ahmed, "Overcoming chromatic dispersion effects in fiber-wireless systems incorporating external modulators," *IEEE Trans. Microwave Theory Tech.,* vol. 45, pp.1410-1415, 1997.

[2] A. Narasimha, X. Meng, M. Wu, and E. Yablonovitch, "Tandem single-side band modulation scheme for doubling spectral efficiency of analogue fiber links," *Electron. Lett.*, vol. 36, pp.1135-1136, 2000.

[3] H. Toda, T. Yamashita, T. Kuri, and K. Kitayama, "Demultiplexing using an arrayed waveguide grating for frequency interleaved DWDM millimeter-wave radio on fiber systems," *J. Lightwave Technol.,* vol.21, pp. 1735-1741, 2003.

[4] X. Zhang, B. Liu, J. Yao, K. Wu, and R. Kashyap, "A novel millimeter-wave band radio over fiber system with dense wavelength division multiplexing bus architecture," *IEEE Trans. Microwave Theory Tech.,* vol. 54, pp. 929-937, 2006.

[5] T. Nakasyotani, H. Toda, T. Kuri, and K. Kitayama, "Wavelength-division multiplexed millimeter-wave band radio on fiber system using a supercontinuum light source," *J. Lightwave Technol.,* vol. 24, pp. 404-410, 2006.

[6] C. Lim, A. Nirmalathas, M. Attyalle, D. Novak, and R. Waterhouse, "On the merging of millimeter-wave fiber radio backbone with 25-GHz WDM ring networks," *J. Lightwave Technol.*, vol. 21, pp. 2203-2210, 2003.

[7] J. Yu, G. Chang, Z. Jia, L. Yi, Y. Su, and T. Wang, "A RoF downstream link with optical mm-wave generation using optical phase modulator for providing broadband optical wireless access service," *OFC 2006, Paper OFM3, CA.*

[8] T. Kuri, H. Toda, and K. Kitayama, "Dense wavelength division multiplexing millimeter wave band radio on fiber signal transmission with photonic downconversion," *J. Lightwave Technol.,* vol. 21, pp. 1510-1517, 2003.

[9] G. Zhou, X. Zhang, J. Yao, K. Wu, and R. Kashyap, "A novel photonic frequency down-shifting technique for millimeter-wave band radio over fiber systems," *IEEE Photonics Technol. Lett.*, vol. 17, pp. 1728-1730, 2005.

[10] A. Kaszubowska, L. Hu, and L. Barry, "Remote downconversion with wavelength reuse for the radio/fiber uplink connection," *IEEE Photonics Technol. Lett.*, vol. 18, pp. 562-564, 2006.

[11] C. Wu and X. Zhang, "Impact of nonlinear distortion in radio over fiber systems with single-side band and tandem single-side band subcarrier modulation," *J. Lightwave Technol.*, vol. 24, pp. 2079-2090, 2006.

[12] B. Masella and X. Zhang, "A novel single wavelength balanced system for radio over fiber links," *IEEE Photonics Technol. Lett.*, vol. 18, pp. 301-303, 2006.

[13] S. Tanaka, N. Taguchi, T. Tsuneto, and Y. Atsumi, "A predistortion-type equi-path linearizer design for radio over fiber system," *IEEE Trans. Microwave Theory Tech.*, vol. 54, pp. 938-944, 2006.

[14] H. Tazawa and W. Steier, "Linearity and ultra-linearization of ring resonator based modulators for sub-octave bandpass analog optical links," *OFC 2006 Paper JThB23, CA.*

[15] D. Deslandes and K. Wu, "Single-substrate integration techniques for planar circuits and waveguide filters," *IEEE Trans. Microwave Theory Tech.*, vol. 51, pp. 593-596, 2003.

[16] J. Simpson, A. Taflove, J. Mix, and H. Heck, "Substrate integrated waveguides optimized for ultrahigh-speed digital interconnects," *IEEE Trans. Microwave Theory Tech.*, vol. 54, pp. 1983-1990, 2006.

[17] A. Patrovsky and K. Wu, "Substrate integrated image guide (SIIG)—a novel planar dielectric waveguide technology for millimeter-wave applications," to appear in *IEEE Trans. Microwave Theory Tech.*, 2006.

[18] F. Xu and K. Wu, "Guided-wave and leakage characteristics of substrate integrated waveguides," *IEEE Trans. Microwave Theory Tech.*, vol. 53, pp. 66-73, 2005.

[19] W. D'Orazio, K. Wu and J. Helszajn, "A substrate integrated waveguide degree-2 circulator," *IEEE Microwave and Wireless Component Lett.*, vol. 14, pp. 207-209, 2004.

[20] Y. Cassivi and K. Wu, "Substrate integrated non-radiative dielectric (SINRD) waveguide," *IEEE Microwave and Wireless Component Lett.*, vol. 14, pp. 89-91, 2004.

[21] J. Dallaire, and K. Wu, "Complete characterization of transmission losses in generalized non-radiative dielectric waveguide," *IEEE Trans. Microwave Theory Tech.*, vol. 48, pp. 121-125, 2000.

[22] N. Grigoropoulos, B. Sanz-Izquierdo, and P. Young, **"**Substrate integrated folded waveguides (SIFW) and filters," *IEEE Microwave and Wireless Component Lett.*, vol. 15, no. 12, pp. 829-831, 2005.

[23] K. Wu, "Towards system-on-substrate approach for future millimeter-wave and photonic wireless applications," *Inter. Joint Conf. Proc. of MINT-MIS/TSMMW*, pp. 229-232, Feb. 2005, Seoul.

[24] D. Deslandes and K. Wu, "Accurate modeling, wave mechanisms, and design considerations of substrate integrated waveguide," to appear in *IEEE Trans. Microwave Theory Tech.*, 2006.